Wave front migration of endothelial cells in a bone-implant interface

Georges Khalil, Sylvie Lorthois, Manuel Marcoux, Pierre Mansat, Pascal Swider

Wave front migration of endothelial cells in a bone-implant interface

Georges Khalil [a], Sylvie Lorthois [a], Manuel Marcoux [a], Pierre Mansat [a,b], Pascal Swider [a,*]

[a] IMFT UMR CNRS 5502, 1 Allées Professeur Camille Soula, 31400 Toulouse, France
[b] Orthopaedic Surgery, Toulouse University Hospital, University of Toulouse, France

Keywords:
Implant fixation
Angiogenesis
Endothelial cells
Growth factor
Reactive transport

A B S T R A C T

The neo-vascularization of the host site is crucial for the primary fixation and the long-term stability of the bone-implant interface. Our aim was to investigate the progression of endothelial cell population in the first weeks of healing. We proposed a theoretical reactive model to study the role of initial conditions, random motility, haptotaxis and chemotaxis in interactions with fibronectin factors and transforming angiogenic factors. The application of governing equations concerned a canine experimental implant and numerical experiments based upon statistical designs of experiments supported the discussion.

We found that chemotaxis due to transforming angiogenic factors was attracting endothelial cells present into the host bone. Haptotaxis conditioned by fibronectin factors favored cells adhesion to the host bone. The combination of diffusive and reactive effects nourished the wave front migration of endothelial cells from the host bone towards the implant. Angiogenesis goes together with new-formed bone formation in clinics, so the similarity of distribution patterns of mineralized tissue observed in-vivo and the spatio-temporal concentration of endothelial cells predicted by the model, tended to support the reliability of our theoretical approach.

1. Introduction

The periprosthetic healing is an intramembranous process, whose outcome is primarily dependent upon the surgical technique (Hahn et al., 1998). Clinically, it is observed that the neo-vascularization of the site plays a key-role in bone tissue formation (Street et al., 2002; Carano and Filvaroff, 2003; Unger et al., 2007) and this evolving process is the consequence of complex mechanobiological events. It is observed that the first days of healing are of prime importance for the survival of the implant fixation.

Endothelial cells are the primary cells involved in angiogenesis. They participate in the construction of the microvasculature, which provides oxygen and nutrients supply and waste elimination. They also contribute to the tissue response by releasing pro-inflammatory factors and by expressing osteoblast adhesion molecules (Peters et al., 2003).

Transforming angiogenic factors (*TAF*) are secreted during the acute inflammatory response. They diffuse and form gradients of growth factors, which initiate chemotactic active migrations of endothelial cells (Terranova et al., 1985; Folkman and Klagsbrun, 1987; Relf et al., 1997; Friedl et al., 1998; Kellar et al., 2001). Major growth factors involved are vascular endothelial growth factors, acidic and basic fibroblast growth factors and angiogenin (Sholley et al., 1984; Terranova et al., 1985; Paweletz and Knierim, 1989; Stokes et al., 1990, 1991; Anderson and Chaplain, 1998; Unger et al., 2007).

The haptotactic response due to adhesion sites and porosity gradients is a consequence of cell interactions with the extracellular matrix. In particular, fibronectin factors (*FF*), which are major component of the matrix (Bowersox and Sorgente, 1982; Quigley et al., 1983; Maheshwari and Lauffenburger, 1998), are particularly implied in this process. It is known that endothelial cells synthesize and secrete *FF* (Birdwell et al., 1978; Jaffee and Mosher, 1978; Macarak et al., 1978; Rieder et al., 1987; Sawada et al., 1987; Bicknell and Harris, 1997; Anderson and Chaplain, 1998; Harrington et al., 2006). This non-diffusive molecule enhances cells adhesion via integrins (Schor et al., 1981; Alessandri et al., 1986; Johansson et al., 1987; Hynes, 1990; Alberts et al., 1994).

Theoretical and numerical models could potentially help interpret complex events associated with angiogenesis. Models of vasculature formation have been proposed for several physiological applications amongst which tumor angiogenesis was a pioneering application (Anderson and Chaplain, 1998; Harrington et al., 2006; McDougall et al., 2006). Other relevant approaches concerned embryo and midbrain morphogenesis (Al-Kilani et al., 2008) and tissue differentiation (Checa and Prendergast, 2009; Geris et al., 2010).

doi:10.1016/j.jbiomech.2011.05.008

Nomenclature

N	endothelial cells.
f	fibronectin factors (*FF*).
c	transforming angiogenic factors (*TAF*).
α_n	endothelial cell proliferation (cell s^{-1}).
λ	rate of *TAF* uptake (mole/cell^{-1} s^{-1}).
μ	rate of *FF* uptake (mole/cell^{-1} s^{-1}).
Ω	source (or sink) terms.
X	coefficient of chemotactic migration (cm^2 mole^{-1} s^{-1}).
D_n, D_f, D_c	coefficient of random diffusion (cm^2 s^{-1}).
h	coefficient of haptotactic migration (cm^2 mole^{-1} s^{-1}).
N_n	cell proliferation threshold (cell mm^3).
ω	rate of *FF* production (M/cell s).
k	adjustment parameter.
∇,Δ	gradient operator, laplacien operator, respectively.

Our aim was to examine the progression of endothelial cell population around an orthopedic implant within the first weeks of healing. We hypothesized that a diffusive and reactive model of endothelial cells population could help rank the role of random motility, haptotaxis and chemotaxis on cells migration. *TAF* and *FF* were considered, the set of governing equations was applied to a canine experimental model (Søballe, 1993) and the discussion was supported by a parametric sensitivity analysis.

2. Material and methods

2.1. Governing equations

The equations of reactive transports was used to model the spatio-temporal behavior of the endothelial cells concentration n, the concentration c of *TAF* and the concentration f of *FF*.

Eq. (1) expressed the cell behavior involving the random motility dependent upon the laplacien of concentration Δn, the chemotaxis related to the *TAF* gradient ∇c and the haptotaxis related to the *FF* gradient ∇f. The coefficient of chemotactic migration $\chi(c)$ was updated using a rational function involving the *TAF* concentration c and the adjustment parameter k. The cell source Ω_n was expressed by a logistic law involving the proliferation coefficient α_n and a proliferation threshold N_n.

$$\frac{\partial n}{\partial t} = D_n \Delta n - \nabla[\chi(c)\nabla c] - \nabla[hn\nabla f] + \Omega_n(n) \tag{1}$$

with $\chi(c) = \chi_0 k/(k+c)$ and $\Omega_n(n) = \alpha_n n(N_n - n)$.

The *TAF* concentration predicted by Eq. (2) involved a diffusive term associated with the laplacien of concentration Δc and a sink term Ω_c to model the *TAF* uptake by endothelial cells.

$$\frac{\partial c}{\partial t} = D_c \Delta c + \Omega_c(n,c) \quad \text{with} \quad \Omega_c(n,c) = -\lambda nc \tag{2}$$

Eq. (3) governed the phase of *FF*. The random diffusion was described by the laplacien of concentration Δf while the source term was involving the secretion factor ω and the uptake factor μ due to cell activity.

$$\frac{\partial f}{\partial t} = D_f \Delta f + \Omega_f(n,f) \quad \text{with} \quad \Omega_f(n,f) = \omega n - \mu nf \tag{3}$$

2.2. Application to an experimental canine implant

The theoretical model was applied to a stable canine implant schematically described in Fig. 1a (Søballe, 1993). With this implant, histological studies showed that the distribution pattern of new-formed tissue was most of the time characterized by a polar symmetry around the implant z-axis (Vestermark et al., 2004). Accordingly, we evaluated our model in the transverse plane intersecting the implant, the post-operative gap and the host bone. As shown in Fig. 1b, the region of interest was delimited by the implant radius $r_i = 3.25$ mm, the drill-hole radius $r_d = 4.1$ mm and the trabecular bone radius $r_s = 7$ mm ($\approx 2 \times r_i$). The post-operative gap was between r_i and r_d and that the host bone was between r_d and r_s.

Neumann boundary conditions were joined to the set of differential Eqs. (1)–(3). As expressed by Eqs. (A.1a) and (A.1b) in the supplementary appendix, the cell gradient and the *FF* gradient were zero at the implant surface. In return, the secretion of *TAF* by local inflammatory cells was expressed by Eq. (A.1c) in the supplementary appendix. At the drill hole, the continuity was described by Eqs. (A.2a), (A.2b) and (A.2c) in supplementary appendix for cells, *FF* and *TAF*, respectively. Into the host bone, the continuity was given by Eqs. (A.3a) and (A.3b) for cells and *FF*, respectively, and the *TAF* gradient was zero as expressed by Eq. (A3c).

The set of continuous governing equations associated with boundary conditions and initial conditions was implemented into Comsol Multiphysics® and solved using a spatio-temporal finite element method. Nodal variables were the endothelial cell fraction n, the *TAF* concentration c and the *FF* concentration f. The meshing shown in Fig. 1b was made of 51,968 quadratic triangular elements, 26,272 mesh points and 313,536 degrees of freedom. The number of boundary elements was 2368, the number of vertex elements was 12 and the minimum element quality was 0.502 with an element aspect ratio of 0.002.

2.3. Statistical experimental design: numerical experimentation

There is a significant level of uncertainty regarding the assignment of parameter values to represent in-vivo conditions, particularly when biologic and mechanical conditions are combined. Therefore, we implemented a parametric sensitivity analysis to elucidate how clinical and biochemical parameters were

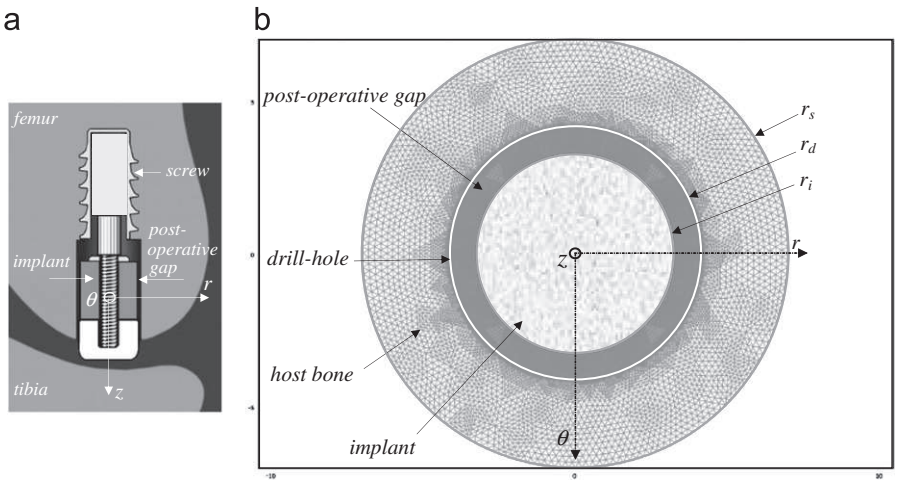

Fig. 1. (a) Description of the canine experimental model. (b) The FE meshing was located in the transverse plane (O, r, θ) of the implant. The concentric zones of interest were the implant surface ($r_i = 3.25$ mm), the post-operative gap ($r_i \le r \le r_d$), and the host bone ($r_d \le r \le r_s$) with $r_d = 4.1$ mm and $r_s = 7$ mm.

influencing endothelial migrations in the periprosthetic zone. We focused on two output measures: (1) the elapsed time t_i for the cell population to reach the implant surface when coming from the host bone and (2) the distribution pattern of cell concentration $n(r)$ into the periprosthetic tissue. We studied the concentrations c_i, c_d and c_g, at the implant surface, at the drill hole and in the middle r_g of the post-operative gap, respectively.

We implemented two statistical designs of experiments (*DOE*) (Box et al., 2005; Goupy and Creighton, 2009). The first numerical experiment noted DOE_1 addressed the role of initial conditions for endothelial cells, *TAF* and *FF*. The second numerical experiment denoted DOE_2 concerned the role of random motility and active migrations of endothelial cells.

Dimensioned factors expressed by Eq. (A4) in supplementary appendix were represented at three levels: reference level (index *r*), high and low levels noted (+) and (−). Output measures t_i, c_i, c_g and c_d were computed using the reference level and the response was noted $\bar{u}$. High levels (+) and low levels (−) were used to successively compute the new responses noted u. Discrepancies between response u and $\bar{u}$ were expressed as polynomial Eq. (4a) for DOE_1 and (4b) for DOE_2. Coefficients a_1 to a_3 described the first order direct effects of factor variations, coefficients a_4 to a_6 expressed the second order combined effects and a_7 concerned the third order combined effect.

$$u-\bar{u}=a_1n+a_2f+a_3c+a_4nf+a_5nc+a_6fc+a_7nfc \tag{4a}$$

$$u-\bar{u}=a_1D+a_2h+a_3\chi+a_4Dh+a_5D\chi+a_6h\chi+a_7Dh\chi \tag{4b}$$

Interpretation of published data allowed establishing plausible levels of ±25% for *n*, *f*, *c*, *D*, *h* and χ. Reference levels and constant data were as follows: $D_n=10^{-9}$ cm^2/s, $D_f=2\times10^{-7}$ cm^2/s, $D_c=2.9\times10^{-7}$ cm^2/s , $\chi_r=2600$ cm^2/s mole, $h_r=900$ cm^2/s mole, $\alpha_n=1.9\times10^{-10}$ cell/s, $N_n=1000$ cell mm^3, $\lambda=725\times10^{-25}$ moles/cell s, $\omega=362\times10^{-25}$ mole/cell s, $\mu=725\times10^{-25}$ mole/cell s and $k=2.9\times10^{-10}$. Data were retrieved from literature (Lauffenburger et al., 1984; Puleo et al., 1991; Linkhart et al., 1996; Maheshwari and Lauffenburger, 1998; Anderson and Chaplain, 1998; Dee et al., 1999; Tranqui and Tracqui, 2000; Conover, 2000; Bailon-Plaza and Van der Meulen, 2001).

The initial conditions of the *TAF* concentration were $c_0=10^{-10}$ moles at the implant surface and zero elsewhere. The initial concentration of *FF*, lower than that of *TAF*, was $f_0=7.5\times10^{-11}$ moles in the host bone and zero in the post-operative gap. The initial concentration of endothelial cells was $n_0=1000$ into the host bone and zero into the gap. Finally, the angiogenic process was computed up to five weeks postoperatively.

3. Results

3.1. Spatio-temporal distribution patterns

Initially, the evolution with time of endothelial cell concentration *n*, *TAF* concentration *c* and *FF* concentration *f* were computed using the reference level of input data. Results plotted in Fig. 2 showed the transient response obtained at the implant surface r_i, into the post-operative gap r_g and at the drill hole r_d. As shown in Fig. 2a, the highest concentration of *TAF* was found in the vicinity of the implant within the first days (point 1). Into the gap, the concentration was maximum in about six days (point 2). At the drill hole, it was converging at five weeks (point 3). Fig. 2b showed the simultaneous increase in *FF* both at the implant surface and into the gap. An acceleration of *FF* formation was found at the drill hole within the first days of healing (point 1). Convergence was nearly reached at five weeks (point 2). Fig. 2c highlighted the time delay of cell concentrations at the drill hole (point 1), into the gap (point 2) and at the implant surface (point 3). Increased rates were similar to reach point 4, point 5 and point 6 showing the maximum concentration obtained at the implant surface at five weeks.

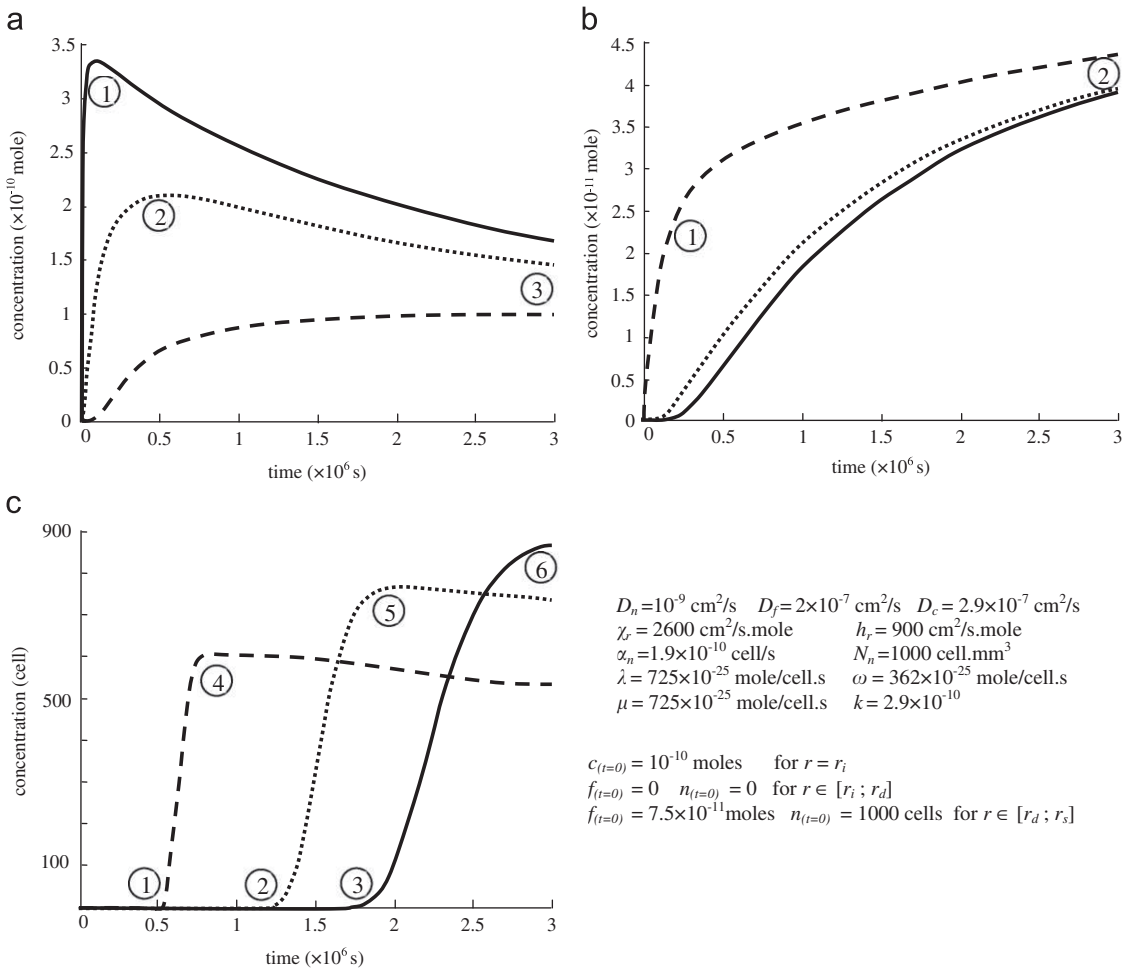

Fig. 2. Evolution with time of concentrations in the periprosthetic zone. (a) Transforming growth factors (*TAF*, variable *c*), (b) Fibronectin factors (*FF*, variable *f*), (c) Endothelial cells population (variable *n*). Concentrations computed with the reference value of input data were plotted at the implant surface (–r_i=3.25 mm), into the post-operative gap (• • • • r_g=3.5 mm) and at the drill-hole (– – r_d=4.1 mm).

Fig. 3 showed the radial distribution patterns of *TAF*, *FF* and endothelial cells, respectively, at five, 10 and 35 days postoperatively. *TAF* diffused towards the host bone and the concentration was divided by two at the implant surface after five weeks. At the same time, *FF* showed a significant increase at the implant surface since starting from zero, a concentration of 4×10^{-11} moles was found. After five weeks, *TAF* and *FF* showed monotonic distribution patterns whereas a wave front migration of cells from the host bone towards the implant was predicted. At ten days, the population peak was located at mid-gap and developed an oscillation. At twenty days, the endothelial cells reached the implant and at thirty-five days, the cell concentration was significant as shown in Fig. 3b. We noted that the oscillation was increasing with time.

3.2. Numerical experimentation

3.2.1. Influence of initial conditions on endothelial cells: DOE_1

Eq. (5) and associated bar diagrams in Fig. 4 were the image of DOE_1 governed by Eq. (4a). The algebraic sign of a_i indicated whether the effect was favorable (+) or unfavorable (−) to the magnitude of output measures: the time t_i for the cell wave front to reach the implant and the cell concentrations n_d at the drill hole, n_g into the gap and n_i at the implant surface, five weeks post-operatively.

$$t-\bar{t} = -0.43n+0.72f-1.45c+0.14nf+0.29nc+0fc-0.58nfc \quad (5a)$$

$$n_i-\bar{n}_i = 106n+18f+180c+28nf+71nc+5.8fc-1.67nfc \quad (5b)$$

$$n_g-\bar{n}_g = 147.5n-9.16f+42.5c-6.67nf+14.16nc+9.16fc-5.83nfc \quad (5c)$$

$$n_d-\bar{n}_d = 177.5n-8.33f-35c+14.17nf+15.83nc+33.33fc-53.33nfc \quad (5d)$$

At the first order, Eq. (5a) and Fig. 4a showed that the initial concentration of cells in the host bone ($a_1=-0.43$) and the initial concentration of *TAF* at the implant surface ($a_3=-1.45$) were reducing the time propagation of cell wave front. In return, the initial concentration of *FF* played a delaying role ($a_2=0.72$) while favoring adhesion to the host bone. Second order combined

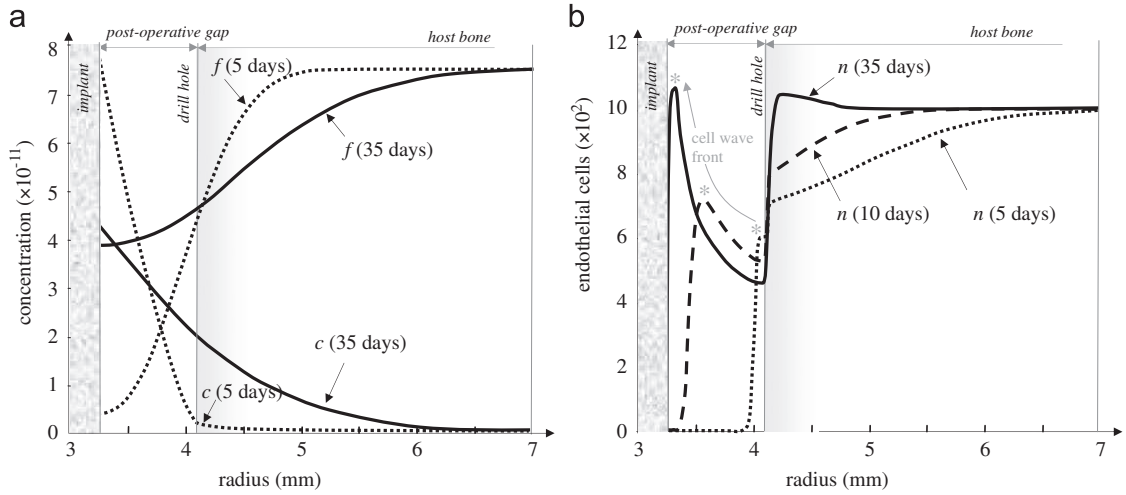

Fig. 3. Radial distribution patterns of endothelial cells, transforming angiogenic factors (*TAF*) and fibronectin factors (*FF*) at five days (• • • •), 10 days (– –) and 35 days (–) post-operatively. Results were obtained with reference levels of input data listed in Fig. 2. (a) *TAF* (variable *c*) and *FF* (variable *f*). (b) endothelial cells (variable *n*). The cell wave front was plotted by symbol *.

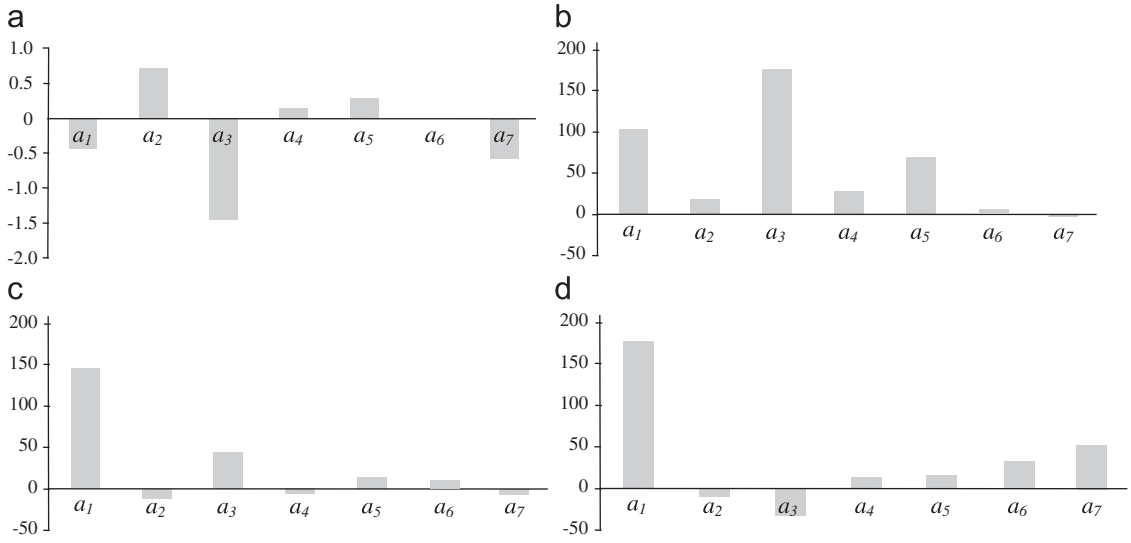

Fig. 4. Influence of initial conditions on the prediction of endothelial cell population at five weeks post-operatively: DOE_1. Bar diagrams plotted coefficients a_i of Eqs. (5a)–(5d). (a) time *t* for endothelial cell wave front to reach the implant ($ri=3.25$ mm), (b) cell concentration n_i at the implant ($ri=3.25$ mm), (c) cell concentration n_g into the post-operative gap ($r_g=3.5$ mm) and (d) cell concentration n_d at the drill-hole ($r_d=4.1$ mm).

effects were delaying and it was found that the third order combined effect (-0.58) had also noticeable influence on the cell wave front migration.

Eqs. (5b) and (5c) and Fig. 4b and c showed that initial concentrations of cells in the host bone and *TAF* at the implant surface had predominant and favorable effects on the final cell concentration at the implant surface ($a_1=106$, $a_3=180$) and into the gap ($a_1=147.5$, $a_3=42.5$). Eq. (5d) and Fig. 4d showed that the initial presence of cells in the host bone was predominant to explain the cells concentration ($a_1=177.5$) at the drill hole after five weeks. In return, the combined effects of initial cells, *TAF* and *FF* (-53.33) tended to decrease this concentration.

3.2.2. *Influence of random motility and active migrations on endothelial cells: DOE_2*

Eq. (6) and associated bar diagrams in Fig. 5 were the image of DOE_2 governed by Eq. (4b). We studied the influence of random motility, haptotaxis due to *FF* and chemotaxis due to *TAF*, on cell wave front migration and cell concentrations at the drill hole, into the gap and at the implant surface, five weeks postoperatively.

$$t-\bar{t}=-2D+0.29h-2\chi+0.29Dh+0.87D\chi-0.58h\chi+0Dh\chi \quad (6a)$$

$$n_i-\bar{n}_i=-10D-35h+142.5\chi+2.5Dh-15D\chi-2.5h\chi+15Dh\chi \quad (6b)$$

$$n_g-\bar{n}_g=-16.25D-7h+25\chi+0.42Dh+15.83D\chi+8.33h\chi-14.16Dh\chi \quad (6c)$$

$$n_d-\bar{n}_d=6.25D-8.75h-42.5\chi-3.75Dh+0D\chi+5h\chi+0Dh\chi \quad (6d)$$

Eq. (6a) and Fig. 5a showed that the cell random motility or diffusion ($a_1=-2$) and chemotaxis ($a_3=-2$) had major effects on cell wave front migration and they shortened time propagation from the host bone toward the implant. Eq. (6b) and Fig. 5b showed that chemotaxis was preponderant ($a_3=142.5$) to explain the cell presence on the implant surface after five weeks. In the post-operative gap, chemotaxis was present ($a_3=25$) but its favorable influence was counteracted by the random motility ($a_1=-16.25$) and haptotaxis ($a_2=-7$, $a_7=-14.16$), as shown in Eq. (6c) and Fig. 5c. Eq. (6d) and Fig. 5d showed that chemotaxis was significantly decreasing the cell concentration at the drill hole ($a_3=-42.5$). Other direct effects and combined effects played minor roles.

4. Discussion and conclusion

We proposed a reactive model to predict the migration of endothelial cells in a bone-implant interface. The theory inspired by works in implant fixation (Ambard and Swider, 2006; Guérin et al., 2009) and tumors angiogenesis (Anderson and Chaplain, 1998) was completed by source terms to take into account the proliferation and diffusive terms to enhance the prediction of growth factor migrations. It was applied to a canine experimental model and extended by a parametric sensitivity analysis.

Amongst the biochemical factors present into the blood clot after surgery, we assumed that the most relevant ones were vascular endothelial growth factors for chemotaxis and proliferation and fibronectin factors for adhesion (Anderson and Chaplain, 1998; Unger et al., 2007). The theoretical methodology could have been applied to other factors provided that constitutive laws were available.

TAF were secreted during the acute inflammatory response due to surgery (blood clot). They formed concentrations into the post-operative gap and they found favorable conditions to attach to the implant surface. They diffused towards the host bone, favored cell proliferation and induced cell chemotactic migration towards the implant.

Initial *FF* diffused from the host bone and their balance was modified because of secretion and uptake by endothelial cells. Diffusion characteristic times of *FF* and *TAF* were lower than that of cell motility. Finally, the combination of diffusive and reactive effects nourished a wave front migration of endothelial cells from the host bone to the implant.

The cells found favorable conditions while migrating towards the implant surface but *TAF* were chemical species that diffused and their source was not endless. Adhesion gradients due to *FF* were always present at the drill hole. As a result, the concentration showed a local peak in the vicinity of the implant surface and

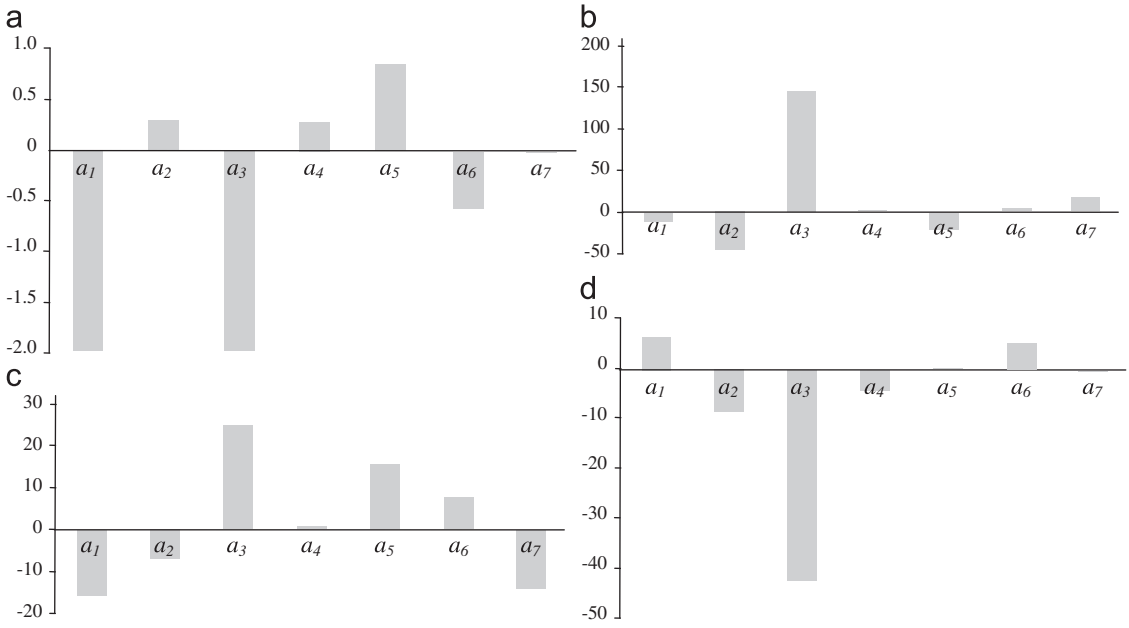

Fig. 5. Influence of random motility and active migrations on endothelial cell population: DOE_2. Bar diagrams plotted coefficients a_i of Eqs. (6a)–(6d). (a) Time t for endothelial cell wave front to reach the implant ($ri=3.25$ mm), (b) cell concentration n_i at the implant ($ri=3.25$ mm), (c) cell concentration n_g into the post-operative gap ($r_g=3.5$ mm) and (d) cell concentration n_d at the drill-hole ($r_d=4.1$ mm).

a decrease into the gap. If there were no *TAF* in the post-operative gap, then the cell migration would have been inhibited.

The sensitivity analysis showed that chemotaxis due to *TAF*, and random diffusion, although counteracted by the haptotactic effects of FF, were playing a predominant role in the endothelial cell migration.

The parameters were all constant in time while they could have evolved with the formation of extracellular matrix within the tissues. While some updating could be made with bony tissue (Ambard and Swider, 2006), convective and diffusive properties of vascular tissue were poorly known especially in bone neo-vascularization. This showed that mixed theoretical-experimental studies, in-vitro and in-vivo, could be planned to reinforce the model relevance.

We found that initial conditions assigned to the theoretical model were playing a major role although they were questionable, and we met known limitations of mathematical models when applied to clinical contexts. We had no quantified data about tissue diffusive properties and initial concentrations even if the canine experimental model was well documented on other aspects.

Our choices were inspired from literature (Bailon-Plaza and Van der Meulen, 2001; Anderson and Chaplain, 1998). They aimed at reproducing clinical observations in implant fixation within the restrictive set of governing equations. A first assumption was set indicating that concentrations of endothelial cells and *FF* were more present in the host bone rather than into the post-operative gap. Secondly, the concentration of chemotactic factors was close to zero after the surgery except in the vicinity of the implant. The initial diffusion due to inflammatory cells was developing an attractive activity. We found that cells and *TAF* were predominant at the first order to interpret the angiogenic process with our modeling, but it appeared that the combined effects of three parameters: cells, *TAF* and *FF* brought a noticeable contribution. This combination was also shortening the time for cells to reach the implant surface as *TAF* did but it decreased the neo-vascularization at the drill-hole in opposition with the first order effect of cells. Finally, numerical experiments confirmed that the initial amounts of cells, *TAF* and *FF* were modifying the magnitude of output measures of the mathematical model but the wave front migration did not have to be reconsidered.

Qualitatively, our findings were consistent with previous studies that highlighted the significant effects of biochemical factors on the endothelial cells migration and proliferation especially in predictive models of tumors (Anderson and Chaplain, 1998; Harrington et al., 2006) or applications in tissue engineering (Unger et al., 2007). Implementing quantitative comparisons was challenging because of specificities of physiological sites and pathologies, uncontrolled biochemical factors or unknown mechanobiological stimuli. Nevertheless, characteristic times of cell wave front migration in our model were of the same order of previously cited works (Anderson and Chaplain, 1998).

The endothelial cells participated in the construction of the microvasculature, which provides oxygen, nutrients supply, waste elimination, release of pro-inflammatory factors and expression of osteoblast adhesion molecules. Therefore, the neo-vascularization goes together with new-formed bone formation (Raines et al., 2010; Santos and Reis, 2010) and clinically, this point is of particular interest to enhance the primary and long-term fixation of implants (Davies, 2003; Broos and Sermon, 2004; Sakka and Coulthard, 2009).

With our canine experimental model, histological studies showed that several types of distribution patterns of neo-formed bone could be found, and all involved peaks in the drill-hole zone and at the implant surface (Vestermark et al., 2004; Ambard and Swider, 2006; Swider et al., 2010). Unfortunately, studies about the neo-vascularization and the activity of endothelial cells have not been carried out yet. These are planned in our further experiments.

With the theoretical model, the wave front migration of endothelial cells showed time-dependent oscillations with maximal discrepancies at the drill-hole and at the implant surface. With the canine experimental model, we also found concentration of mineralized tissue at the drill-hole zone (condensed bone rim) and at the implant surface. Given that the population of endothelial cells was a major actor of bone formation, the similarity of distribution patterns corroborated the relevance of our theoretical model.

Mechanobiological events played a significant role in tissue formation. In a first step, our theoretical model referred to the stable and unloaded canine implant and no mechanical loads were taken into account. We are currently implementing a more complete model with mechanical stimuli (micromotion and shear) to mimic in-vivo conditions related to loaded unstable implants.

In conclusion, aware of correlations between neo-vascularization and implant fixation, our theoretical and numerical modeling could potentially be exploited to reduce empirical aspects in therapeutic strategies for arthroplasty.

Conflict of interest statement

The authors hereby declare to have no conflict of interest.

Acknowledgment

J.E. Bechtold PhD and Professor K. Søballe MD PhD.

Appendix A. Supplementary material

Supplementary data associated with this article can be found in the online version at doi:10.1016/j.jbiomech.2011.05.008.

References

Al-Kilani, A., Lorthois, S., Nguyen, T.H., Le Noble, F., Cornelissen, A., Unbekandt, M., Boryskina, O., Leroy, L., Fleury, V., 2008. During vertebrate development, arteries exert a morphological control over the venous pattern through physical factors. Phys Rev E Stat. Nonlinear Soft. Matter Phys. 77 (5 Pt 1), 051912.

Alberts, B., Bray, D., Lewis, J., Raff, M., Roberts, K., Watson, J.D., 1994. The Molecular Biology of the Cell, 3rd ed. Garland Publishing, New York, USA.

Alessandri, G., Raju, K.S., Gullino, P.M., 1986. Interaction of gangliosides with fibronectin in the mobilization of capillary endothelium. Possible influence on the growth of metastasis. Invasion Metastasis 6, 145–165.

Ambard, D., Swider, P., 2006. A predictive mechano-biological model of the bone-implant healing. Euro. J. Mech.—A/Solids 25 (6), 927–937.

Anderson, A.R.A., Chaplain, M.A.J., 1998. Continuous and discrete mathematical models of tumor-induced angiogenesis. Bull. Math. Biol. 60, 857–900.

Bailon-Plaza, A., Van der Meulen, M.C., 2001. A mathematical framework to study the effects of growth factor influences on fracture healing. J. Theor. Biol. 212 (2), 191–209.

Bicknell, R., Harris, A.L., 1997. Expression of the angiogenic factors vascular endothelial cell growth factor, acidic and basic fibroblast growth factor, tumor growth factor beta-1, platelet-derived endothelial cell growth factor, placenta growth factor, and pleiotrophin in human primary breast cancer and its relation to angiogenesis. Cancer Res. 57 (5), 963–969.

Birdwell, C.R., Gospodarowicz, D., Nicolson, G.L., 1978. Identification, localization and role of fibronectin in cultured endothelial cells. Proc. Natl. Acad. Sci. USA 75, 3273–3277.

Bowersox, J.C., Sorgente, N., 1982. Chemotaxis of aortic endothelial cells in response to fibronectin. Cancer Res. 42, 2547–2551.

Box, G.E.P., Hunter, W.G., Hunter, J.S., 2005. Statistics for experimenters: design, innovation, and discovery, 2nd ed. Wiley & Sons, New York.

Broos, P.L., Sermon, A., 2004. From unstable internal fixation to biological osteosynthesis. A historical overview of operative fracture treatment. Acta Chir. Belg. 104 (4), 396–400.

Carano, R.A., Filvaroff, E.H., 2003. Angiogenesis and bone repair. Drug Discovery Today 8 (21), 980–989 (review).

Checa, S., Prendergast, P.J., 2009. A mechanobiological model for tissue differentiation that includes angiogenesis: a lattice-based modeling approach. Ann. Biomed. Eng. 37 (1), 129–145.
Conover, C.A., 2000. Insulin-like growth factors and the skeleton. In: Canalis, E. (Ed.), Skeletal Growth Factors. Lippincott Williams & Wilkins, Philadelphia, PA, USA, pp. 101–116.
Davies, J.E., 2003. Understanding peri-implant endosseous healing. J. Dent. Educ. 67 (8), 932–949.
Dee, K.C., Anderson, T.T., Bizios, R., 1999. Osteoblast population migration characteristics on substrates modified with immobilized adhesive peptides. Biomaterials 20 (3), 221–227.
Folkman, J., Klagsbrun, M., 1987. Angiogenic factors. Science 235, 442–447.
Friedl, P., Zanker, K.S., Brogcker, E.B., 1998. Cell migration strategies in 3-D extracellular matrix: differences in morphology, cell matrix interactions, and integrin function. Micros. Res. Tech. 43, 369–378.
Geris, L., Vandamme, K., Naert, I., Vander Sloten, J., Van Oosterwyck, H., Duyck, J., 2010. Mechanical loading affects angiogenesis and osteogenesis in an in vivo bone chamber: a modeling study. Tissue Eng. A 16 (11), 3353–3361.
Goupy, J., Creighton, L., 2009. Introduction to Design of Experiments: with JMP Examples, third ed. SAS Press.
Guérin, G., Ambard, D., Swider, P., 2009. Cells, growth factors and bioactive surface properties in a mechanobiological model of implant healing. J. Biomech. 42 (15), 2555–2561.
Hahn, M., Vogel, M., Eckstein, F., Pompesius-Kempa, M., Delling, G., 1998. Bone structure changes in hip joint endoprosthesis implantation over the course of many years. A quantitative study. Chirurg 59 (11), 782–787.
Harrington, H.A., Maier, M., Naidoo, L., Whitaker, N., Kevrekid, P.G., 2006. A hybrid model for tumor-induced angiogenesis in the cornea in the presence of inhibitors. Math. Comput. Model 46, 513–524.
Hynes, R.O., 1990. Fibronectins. Springer-Verlag, New York.
Jaffee, E.A., Mosher, D.F., 1978. Synthesis of fibronectin by cultured endothelial cells. J. Exp. Med. 147, 1779–1791.
Johansson, S., Gustafson, S., Pertoft, H., 1987. Identification of a fibronectin receptor specific for rat liver endothelial cells. Exp. Cell Res. 172, 425–431.
Kellar, R.S., Kleiment, L.B., Williams, S.K., 2001. Characterization of angiogenesis and inflammation surrounding ePTFE implanted on the epicardium. J. Biomed. Mater. Res. 61 (2), 226–233.
Linkhart, T.A., Mohan, S., Baylink, D.J., 1996. Growth factors for bone growth and repair: IGF, TGF beta and BMP. Bone 19 (1 Suppl), 1S–12S (review).
Lauffenburger, D., Aris, R., Kennedy, C.R., 1984. Travelling bands of chemotactic bacteria in the context of population growth. Bull. Math. Biol. 46, 19–40.
Macarak, E.J., Kirby, E., Kirk, T., Kefalides, N.A., 1978. Synthesis of cold-insoluble globulin by cultured calf endothelial cells. Proc. Natl. Acad. Sci. USA 75 (6), 2621–2625.
Maheshwari, G., Lauffenburger, D.A., 1998. Deconstructing (and reconstructing) cell migration. Microsc. Res. Tech. 43, 358–368.
McDougall, S.R., Anderson, A.R.A., Chaplain, M.A.J., 2006. Mathematical modeling of dynamic adaptive tumor-induced angiogenesis: clinical implications and therapeutic targeting strategies. J. Theor. Biol. 241, 564–589.
Paweletz, N., Knierim, M., 1989. Tumor-related angiogenesis. Crit. Rev. Oncol. Hematol. 9, 197–242.
Peters, K., Unger, R.E., Brunner, J., Kirkpatrick, C.J., 2003. Molecular basis of endothelial dysfunction in sepsis. Cardiovasc. Res. 60, 49–57.
Puleo, D.A., Holleran, L.A., Doremus, R.H., Bizios, R., 1991. Osteoblast responses to orthopedic implant materials in vitro. J. Biomed. Mater. Res. 25 (6), 711–723.
Quigley, J.P., Lacovara, J., Cramer, E.B., 1983. The directed migration of B-16 melanoma-cells in response to a haptotactic chemotactic gradient of fibronectin. J. Cell Biol. 97, A450–A451.
Raines, A.L., Olivares-Navarrete, R., Wieland, M., Cochran, D.L., Schwartz, Z., Boyan, B.D., 2010. Regulation of angiogenesis during osseointegration by titanium surface microstructure and energy. Biomaterials 31 (18), 4909–4917.
Relf, M., LeJeune, S., Scott, P.A., Fox, S., Smith, K., Leek, R., Moghaddam, A., Whitehouse, R., Bicknell, R., Harris, A.L., 1997. Expression of the angiogenic factors vascular endothelial cell growth factor, acidic and basic fibroblast growth factor, tumor growth factor beta-1, platelet-derived endothelial cell growth factor, placenta growth factor, and pleiotrophin in human primary breast cancer and its relation to angiogenesis. Cancer Res. 57 (5), 963–969.
Rieder, H., Ramadori, G., Dienes, H.P., Meyer, K.H., 1987. Sinusoidal endothelial cells from guinea pig liver synthesize and secrete cellular fibronectin in vitro. Hepatology 7, 856–864.
Sakka, S., Coulthard, P., 2009. Bone quality: a reality for the process of osseointegration. Implant Dent. 18 (6), 480–485 (review).
Santos, M.I., Reis, R.L., 2010. Vascularization in bone tissue engineering: physiology, current strategies, major hurdles and future challenges. Macromol Biosci. 10 (1), 12–27 (review).
Sawada, H., Furthmayr, H., Konomi, H., Nagai, Y., 1987. Immuno electron microscopic localization of extracellular matrix components produced by bovine corneal endothelial cells in vitro. Exp. Cell Res. 171, 94–109.
Schor, S.L., Schor, A.M., Brazill, G.W., 1981. The effects of fibronectin on the migration of human foreskin fibroblasts and syrian hamster melanoma cells into three-dimensional gels of lattice collagen fibres. J. Cell Sci. 48, 301–314.
Sholley, M.M., Ferguson, G.P., Seibel, H.R., Montour, J.L., Wilson, J.D., 1984. Mechanisms of neovascularization. Vascular sprouting can occur without proliferation of endothelial cells. Lab. Invest. 51 (6), 624–634.
Søballe, K., 1993. Hydroxyapatite ceramic coating for bone implant fixation. Mechanical and histological studies in dogs. Acta Orthop. Scand. Suppl. 255, 1–58 (review).
Stokes, C.L., Rupnick, M.A., Williams, S.K., Lauffenburger, D.A., 1990. Chemotaxis of human microvessel endothelial cells in response to acidic fibroblast growth factor. Lab. Invest. 63, 657–668.
Stokes, C.L., Lauffenburger, D.A., Williams, S.K., 1991. Migration of individual microvessel endothelial cells: stochastic model and parameter measurement. J. Cell Sci. 99, 419–430.
Street, J., Bao, M., deGuzman, L., Bunting, S., Peale Jr, F.V., Ferrara, N., Steinmetz, H., Hoeffel, J., Cleland, J.L., Daugherty, A., van Bruggen, N., Redmond, H.P., Carano, R.A., Filvaroff, E.H., 2002. Vascular endothelial growth factor stimulates bone repair by promoting angiogenesis and bone turnover. Proc. Natl. Acad. Sci. USA 23;99 (15), 9656–9661.
Swider, P., Ambard, D., Guerin, G., Søballe, K., Bechtold, J.E., 2010. Sensitivity analysis of periprosthetic healing to cell migration, growth factor and post-operative gap using a mechanobiological model. Comput. Methods Biomech. Biomed. Eng. 2010 Nov 15:1. Nov 15:1. [Epub ahead of print].
Tranqui, L., Tracqui, P., 2000. Mechanical signalling and angiogenesis. The integration of cell-extracellular matrix couplings. C.R. Acad. Sci. Ser. III 323 (1), 31–47.
Terranova, V.P., Diflorio, R., Lyall, R.M., Hic, S., Friesel, R., Maciag, T., 1985. Human endothelial cells are chemotactic to endothelial cell growth factor and heparin. J. Cell Biol. 101, 2330–2334.
Unger, R.E., Sartoris, A., Peters, K., Motta, A., Migliaresi, C., Kunkel, M., Bulnheim, U., Rychly, J., Kirkpatrick, C.J., 2007. Tissue-like self-assembly in co cultures of endothelial cells and osteoblasts and the formation of microcapillary-like structures on three-dimensional porous biomaterials. Biomaterials 28, 3965–3976.
Vestermark, M.T., Bechtold, J.E., Swider, P., Søballe, K., 2004. Mechanical interface conditions affect morphology and cellular activity of sclerotic bone rims forming around experimental loaded implants. J. Orthop. Res. 22 (3), 647–652.